ELSEVIER

Journal of Fluorine Chemistry 90 (1998) 9–16

JOURNAL OF FLUORINE CHEMISTRY

A computer modelling study on the interaction of $-(CF_2CF_2O)-$ polyperfluorinated ethers with Lewis acid sites: perfluorodiethyl ether

R.J. Waltman *

IBM Storage Systems Division, 5600 Cottle Road, San Jose, CA 95193, USA

Received 14 July 1997; accepted 18 December 1997

Abstract

Lewis acid catalysis significantly enhances the thermally induced degradation of polyperfluorinated ether lubricants. We have used $CF_3CF_2OCF_2CF_3$ and AlF_3 as models to investigate via ab initio theory, the Lewis acid–base interactions between polyperfluorinated ethers and Lewis acid sites. The results of these studies indicate that perfluorodiethyl ether, or PFDEE, may form a Lewis acid–base pair between the ether oxygen atom in PFDEE and the aluminum atom in AlF_3 provided that there is no steric hindrance limiting access to the ether oxygen atom. This may be achieved, for example, by PFDEE adopting a trans–gauche instead of a trans–trans conformation. In the trans–trans conformation, a terminal perfluoromethyl group sterically interferes with the accessibility of the ether oxygen atom to the AlF_3 surface. These results indicate that in lubricant molecules such as the 'Z' family of Fomblin fluids, composed of a copolymer of perfluoromethylene and perfluoroethylene oxide units, steric hindrance will limit AlF_3 access to the ether oxygen atom and would depend upon the ratio of $-CF_2CF_2O$ and $-CF_2O-$ structural units and their spatial distribution. Even when the $-CF_2CF_2OCF_2CF_2-$ PFDEE backbone adopts a local trans–gauche conformation such as to spatially allow a Lewis acid–base interaction between the ether oxygen atom and aluminum, the interatomic distance is much greater, 2.5 Å compared to 1.8 Å for perfluoromethylene oxide. The binding energy is correspondingly smaller, −3 compared to −9 kcal/mol, respectively. Several degradation paths for the decomposition of PFDEE, originating within the $-CF_2OCF_2-$ structural group, were computed. Thus, the decomposition of PFDEE to CF_3CF_3 and CF_3CFO via an initial cleavage of a C–O bond, and, alternatively, via a transition state, were investigated. In both cases, the activation energy to initiate the decomposition is rather high, near 80–100 kcal/mol. However, in the presence of an AlF_3 catalyst, the activation energy for the decomposition reaction via the transition structure is significantly reduced to 50 kcal/mol. Alternatively, a C–O bond scission leading to the formation of radical sites adjacent to $-CF_2O-$ structural units may lead to mass loss via elimination of COF_2. Such a reaction proceeds with an activation energy of only 24 kcal/mol.

Keywords: Lewis acid; Perfluorodiethyl ether; Trans–gauche conformation

1. Introduction

Polyperfluorinated ethers (PPFE) are viscous liquids that are commonly used in the magnetic recording industry as topical lubricants for rigid magnetic media, or computer disks. They, together with the hard carbon overcoat, provide the necessary protection of the underlying magnetic film against damage due to wear caused by head–disk contacts during operation of the drive. Thus, it is imperative that a PPFE lubricant be selected that will sustain this protective action for the lifetime of the drive. There are more than several factors that must be considered to ensure such success. First, current hard disk drives typically operate at elevated temperatures near 45–60°C, hence knowledge of the thermal response of the lubricant on the computer disk, and all of its subsequent consequences, such as evaporation, bonding to the disk, and changes in surface energy, is important [1]. Second, lubricant degradation in the disk drive must be minimized by suitable choice of the PPFE lubricant, and both the choice of backbone and end group(s) play a definitive role [2–6]. In this report, we are concerned primarily with the degradation of PPFE induced by Lewis acid sites. Our motivation for this work originates from the experimental observation that the degradation of PPFE is catalyzed by AlF_3 [2–6]. Al_2O_3 is often present in magnetic recording media and/or slider in the α form. XPS studies have shown that such surfaces, when in contact with PPFE lubricants, eventually incorporate fluorine into the Al_2O_3 surface corresponding to fluorine in AlF_3 [2–4]. Kasai and Wheeler [2], Kasai [3], and Kasai et al. [4] have further demonstrated that PPFE lubricants, in particular with the $-CF_2O-$ structural moiety,

* Corresponding author. Tel.: +1-408-256-0475.

0022-1139/98/$19.00
PII S0022-1139(98)00141-9

Table 1
Some optimized parameters

Structure	Total E	ZPE	U	S	Imag freq
PFDEE (Fig. 1a)	−1220.749116	41.26696	49.121	114.917	0
PFDEE–AlF_3 (Fig. 1b)	−1761.212500	47.27309	58.798	144.168	0
PFDEE–AlF_3 (Fig. 1c)	−1761.205057	47.38088	58.866	142.830	0
PFDEE–TS (Fig. 2a)	−1220.587334	38.97551	46.881	114.116	−357.51
PFDEE–AlF_3–TS (Fig. 2b)	−1761.119003	46.17792	57.515	141.348	−79.67
AlF_3	−540.450452	5.250	7.952	69.264	0
CF_3CFO	−548.357351	18.552	22.144	78.558	0
CF_3CF_3	−672.384482	20.678	24.678	81.473	0
$CF_3CF_2^{\bullet}$	−572.877120	17.242	20.920	80.349	0
$CF_3CF_2O^{\bullet}$	−647.750740	20.140	24.245	83.711	0
$CF_3\cdots CF_2O^{\bullet}$ (Fig. 4)	−647.708644	18.075	22.474	86.865	−1033.08
COF_2	−311.615306	9.907	11.907	61.456 0	
$CF_3^{\bullet}$	−336.128946	8.525	10.615	65.009	0

Total E is the total energy (hartree); ZPE is the zero-point energy (kcal/mol); U is the internal energy (kcal/mol, 298 K); S is the entropy (cal/mol K, 298 K); Imag freq is the imaginary frequency (cm^{-1}, unscaled) where a zero indicates no imaginary frequency is computed. All open shell molecules were computed using spin restricted ROHF method, except for the Fig. 4 structure where UHF was used.

undergo vigorous decomposition in the presence of Al_2O_3, AlF_3, and $AlCl_3$. Since the structure of the converted Al_2O_3 surface is unknown, neither is the structural form of AlF_3. Hess and Kemnitz [7] have demonstrated that the α form of AlF_3 reveals no Lewis acid centers and therefore is catalytically inactive while the β form reveals Lewis acidity and hence, catalytic activity.

Previous papers in the series examined the degradation of polyperfluorinated ethers containing the perfluoromethylene oxide, $-CF_2O-$, monomer unit [8,9]. Thus, the reaction coordinates for the decomposition of perfluorodimethyl ether, $F-(-CF_2O-)-CF_3$, to COF_2 and CF_4 were investigated via ab initio theory. These studies revealed that the ether oxygen in perfluorodimethyl ether was sterically accessible to the AlF_3 surface and formed a Lewis acid–base pair with a binding energy of −9 kcal/mol. In the presence of the AlF_3 Lewis acid catalyst, the activation energy for decomposition to products was significantly reduced from 100 to 50 kcal/mol. We now extend these studies to perfluorinated ethers containing the perfluoroethylene oxide, $-CF_2CF_2O-$, monomer unit, by investigating the decomposition of perfluorodiethyl ether, $F-(-CF_2CF_2O-)-CF_2CF_3$. Both the perfluoromethylene and -ethylene oxide monomer units comprise the 'Z' family of polyperfluorinated ethers widely used in the computer industry as a topical lubricant. The results of this investigation will show that the binding energy between the ether oxygen and the aluminum atoms is only −3 kcal/mol. The origin of the smaller binding energy is attributed to steric hindrance provided by one of the terminal perfluoromethyl substituents. Thus, the Lewis acid–base interaction with the ether oxygen atom occurs more readily when PFDEE is in the trans–gauche compared to a trans–trans conformation. In addition, the reaction coordinate for the decomposition of PFDEE to perfluoroacetaldehyde and perfluoroethane is investigated. Both a C–O bond scission to form radicals, and separately, decomposition via an intermolecular fluorine atom transfer within the $-CF_2OCF_2-$ group, are considered. A transition structure leading to the decomposition reaction is identified, having an activation energy of 99 kcal/mol. Catalysis via a Lewis acid–base interaction reduces the activation barrier to 50 kcal/mol.

2. Computational method

Ab initio calculations were performed using the Mulliken computer code [10], using IBM RISC 6000 computers. SCF calculations were performed using the 6-31G* basis set [11]. Harmonic vibrational frequencies were calculated by differentiation of the energy gradient at the optimized geometries. No imaginary frequencies were computed at minima; one imaginary frequency at maxima (transition states). These data are summarized in Table 1. In these studies, we employ AlF_3 as a model for a Lewis acid surface site for several reasons. First, its presence is implicated in PPFE lubricant degradation [2–6]. Second, AlF_3 has comparatively few electrons and is a closed shell, rendering the computational studies more tractable. Bulk AlF_3 is octahedrally surrounded by six F atoms. The actual surface may be more ionic, and possibly more coordinately unsaturated than the bulk [7,12].

3. Results and discussion

3.1. The interaction of $CF_3CF_2OCF_2CF_3$ with AlF_3

Studies of the surface reactions of polyperfluorinated ethers on slided computer disks implicate the formation of metal halides in the wear tracks as playing a significant role in inducing catalytic degradation of the PPFE lubricants [7]. Hence, it is imperative that we understand the nature of the interaction between PPFE and metal halides [2–9]. The

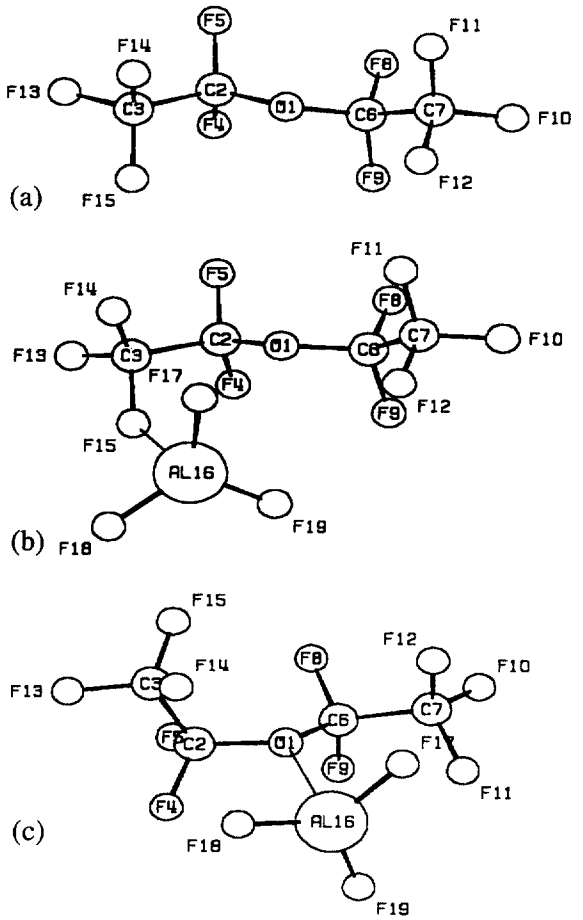

Fig. 1. HF/6-31G* optimized geometries.

results for the geometry optimization of $CF_3CF_2OCF_2CF_3$, hereafter referred to as PFDEE (PerFluoroDiEthyl Ether) are presented in Fig. 1 and Table 2. The structural details for the optimized geometry for PFDEE is consistent with what is already known in the literature from both experimental and theoretical studies [13]. The extended conformation of PFDEE represents the global minimum on the potential energy surface [14]. The most significant result from the theory is that the C–C bonds closest to the C–O–C plane are rotated out of the plane by $\simeq 18°$. This is characteristic of polyperfluorinated ether structures containing the C–O–C backbone and is a result of the interaction between the lone pairs of electrons on the fluorine and oxygen atoms.

In a previous study [9] of the interaction of CF_3OCF_3 with AlF_3, a significant Lewis acid–base interaction developed between the aluminum atom in AlF_3 and the oxygen atom in CF_3OCF_3. A bond distance of 1.83 Å and a binding energy of −9 kcal/mol were computed at SCF/6-31G*. The perfluorodimethyl ether accommodated the AlF_3 surface with no gross structural distortion of the perfluorodimethyl ether backbone. If now we examine the theoretical results for the PFDEE–AlF_3 complex, we observe that the Lewis acid–base interaction between the ether oxygen and aluminum atoms occurs most readily when the PFDEE backbone is near the trans–gauche conformation, and not the extended trans–trans conformation. These structures are presented in Fig. 1. In particular, when the AlF_3 Lewis acid approaches the ether oxygen atom of the trans–trans conformation of PFDEE (Fig. 1a), a terminal perfluoromethyl group sterically interferes with the development of the aluminum–oxygen close contact that leads to the formation of the Lewis acid–base interaction. Instead, the AlF_3 surface 'docks' onto one of the fluorine atoms in the terminal perfluoromethyl group, Fig. 1b, forming an $AlF_3\cdots F$ bridging bond [12]. Conversely, if the trans–trans PFDEE backbone undergoes a C–O internal rotation to produce the trans–gauche conformer, then the steric crowding caused by the terminal perfluoromethyl group may be relieved to the extent that a Lewis acid–base interaction between the ether oxygen and aluminum atoms becomes possible, Fig. 1c.

Let us first consider the complex shown in Fig. 1b, where PFDEE is conformationally extended and the AlF_3 surface has formed a bridging bond to a PFDEE fluorine atom. The F15–Al16 bond distance is 2.11 Å, not unlike the Al···F

Table 2
SCF/6-31G* optimized bond distances (Å), angles (°) and dihedrals (°)

Parameters	PFDEE	PFDEE–AlF_3 Fig. 1c	PFDEE–TS Fig. 2a	PFDEE–TS–AlF_3 Fig. 2b
O1–C2	1.361	1.397	1.239	1.287
O1–C6	1.361	1.386	2.358	2.715
C2–C3	1.529	1.534	1.529	1.529
C2–F4	1.319	1.308	1.340	1.324
C2–F5	1.318	1.311	1.486	1.402
F5–C6	2.962	2.578	2.093	2.329
C6–F8	1.319	1.315	1.248	1.232
C6–F9	1.318	1.312	1.233	1.214
O1–C2–C3	107.96	110.32	118.68	115.13
O1–C2–F4	111.63	107.05	117.80	115.31
O1–C2–F5	110.94	111.41	106.20	106.97
O1–C6–C7	107.96	110.15	78.19	78.43
O1–C6–F8	111.64	110.31	140.17	131.90
O1–C6–F9	110.97	110.05	84.88	77.93
C2–O1–C6	121.42	119.74	95.07	93.25
C2–F5–C6			99.47	108.19
O1–C2–C3–F13	178.98	−173.40	173.73	177.33
O1–C6–C7–F10	178.97	−179.18	174.81	176.19
C2–O1–C6–C7	161.92	169.47	137.52	128.06
C2–O1–C6–F8	41.93	50.28	24.55	12.46
C2–O1–C6–F9	−78.84	−70.10	−98.30	−102.68
C3–C2–O1–C6	161.84	−108.62	−122.50	−127.10
F4–C2–O1–C6	41.84	132.01	105.28	105.15
F5–C2–O1–C6	−78.93	13.04	9.05	13.05
O1–Al16		2.541		1.847
C2–O1–Al16		111.13		134.91
C6–O1–Al16		125.89		
C3–C2–O1–Al16		90.54		101.36
F4–C2–O1–Al16		−28.84		−26.39
F5–C2–O1–Al16		−147.81		−142.15
C7–C6–O1–Al16		−32.73		−87.88
F8–C6–O1–Al16		−151.92		156.52
F9–C6–O1–Al16		87.70		41.39
C–F (CF_3–)	1.31	1.32	1.31	1.31
Al–F (AlF_3–)		1.63	1.65	

bridging distance observed in Al_2F_6 [12]. As a result of the F15–Al16 bond, the C3–F15 bond length in Fig. 1b is 1.36 Å, longer than the nominal 1.31 Å found in PFDEE. The bonds 'gamma' to the F15–Al16 bond, e.g., C2–C3, are very close to the values computed for PFDEE (Table 2) and thus the major structural perturbation as a result of the formation of the Lewis acid–base pair is localized near the bridging site.

In the other complex, Fig. 1c, the Lewis acid–base pair interaction between the ether oxygen and aluminum atoms may be established after an internal rotation to a trans–gauche configuration. In this complex, a rotation of the C3–C2–O1–C6 dihedral angle by approximately 50° allows the oxygen–aluminum close contact to develop. The trans–gauche conformer is 3.0 kcal/mol higher in energy compared to the trans–trans PFDEE geometry, consistent with a previous conformational study of the PFDEE molecule [14]. The O1–Al16 bond distance is 2.54 Å, considerably longer than the 1.83 Å computed for the CF_3OCF_3–AlF_3 complex [9]. This is indicative that the complex remains sterically hindered as a result of the non-bonding close contacts that develop between the fluorine atoms of AlF_3 and of PFDEE: F4–F18 = 2.69 Å; F14–F18 = 2.83 Å; F11–F17 = 2.76 Å; and F12–F17 = 2.87 Å. Hence, an aluminum–oxygen interatomic distance of 2.54 Å is the closest approach possible for the complex shown in Fig. 1c, under these conditions. Consequently, the Lewis acid–base interaction is sterically hindered for perfluoroethylene oxide repeat units. Additional insight may be gathered from a Mulliken population analyses, Table 3. In particular, the O1–Al16 bond order is computed to be 0.061, considerably smaller than the corresponding bond order of 0.138 computed previously for the CF_3OCF_3–AlF_3 complex [9]. There are other noteworthy changes that are induced in the PFDEE backbone as a consequence of the Lewis acid interaction. The C–O bonds 'beta' to the O1–Al16 bond have weakened as a result of the Lewis acid–base interaction. The C–O bond, nominally near 1.36 Å in the uncomplexed Fig. 1a, increases in length to 1.39–1.40 Å. The corresponding C–O bond order decreases by 10% from the nominal 0.855 value. These results indicate that a C–O bond will be more susceptible to scissioning as a consequence of the Lewis acid–base interaction.

The computed partial atomic charges, summarized in Table 4, indicate large partial atomic charges on Al16 and O1 atoms. In PFDEE, the oxygen atom O1 has an excess negative charge of $-0.71\ e^-$ while in AlF_3, Al16 is excessively positive by $+1.70\ e^-$. A comparison of the computed charges in the complex shown in Fig. 1c and PFDEE indicates there is little difference in charge distribution where the structures are similar. The ether oxygen atom O1 retains a large negative partial atomic charge and so the interaction is strongly electrostatic, as expected for a Lewis acid–base.

The binding energies for PFDEE with the AlF_3 surface, Fig. 1, are summarized in Table 5. The binding energies for the complexes shown in Fig. 1b and c are −7.36 and −2.58 kcal/mol, respectively. We note that the aluminum and ether oxygen binding energy for the complex shown in Fig. 1c, −2.58 kcal/mol, is significantly smaller than the corresponding Lewis acid–base interaction between CF_3OCF_3 and AlF_3 investigated previously, where a binding energy of −9.06 kcal/mol was computed [9]. The smaller binding energy computed for the complex shown in Fig. 1c is attributed to the steric hindrance caused by close contacts, as discussed above.

Table 3
SCF/6-31G* computed bond orders

Parameters	PFDEE	PFDEE–AlF_3 Fig. 1c	PFDEE–TS Fig. 2a	PFDEE–TS–AlF_3 Fig. 2b
O1–C2	0.855	0.760	1.396	1.088
O1–C6	0.855	0.787	0.152	0.035
O1–Al16		0.061		0.390
C2–C3	0.985	0.978	0.955	0.975
C2–F4	0.897	0.937	0.865	0.905
C2–F5	0.918	0.920	0.529	0.683
C3–F13	0.941	0.953	0.925	0.933
C3–F14	0.943	0.949	0.936	0.949
C3–F15	0.943	0.948	0.918	0.919
F5–C6	0.002	0.014	0.203	0.102
C6–C7	0.985	0.986	0.925	0.912
C6–F8	0.897	0.907	1.118	1.174
C6–F9	0.918	0.919	1.148	1.247
C7–F10	0.941	0.944	0.912	0.933
C7–F11	0.943	0.931	0.999	1.020
C7–F12	0.943	0.944	0.988	0.996
Al16–F17		0.775		0.740
Al16–F18		0.775		0.742
Al16–F19		0.785		0.675

Table 4
Mulliken partial atomic charges computed at the SCF/6-31G* optimized geometries

Atom	PFDEE	PFDEE–AlF_3 Fig. 1c	PFDEE–TS Fig. 2a	PFDEE–TS–AlF_3 Fig. 2b
O1	−0.711	−0.813	−0.793	−0.885
C2	1.011	1.011	0.945	1.016
C3	1.076	1.081	1.053	1.060
F4	−0.343	−0.324	−0.390	−0.356
F5	−0.339	−0.339	−0.516	−0.474
C6	1.011	1.038	0.916	0.898
C7	1.077	1.085	1.122	1.117
F8	−0.358	−0.353	−0.193	−0.151
F9	−0.352	−0.342	−0.155	−0.088
F10	−0.343	−0.339	−0.349	−0.326
F11	−0.339	−0.329	−0.280	−0.251
F12	−0.339	−0.326	−0.284	−0.275
F13	−0.343	−0.332	−0.358	−0.350
F14	−0.339	−0.329	−0.352	−0.331
F15	−0.339	−0.334	−0.365	−0.358
Al16		1.637		1.560
F17		−0.566		−0.594
F18		−0.566		−0.590
F19		−0.566		−0.623

AlF_3 at SCF/6-31G*: Al +1.699; F −0.563.

Table 5
The relative total energies (6-31G*) for the various structures in kcal/mol

Structure	ΔE
Reactant	
PFDEE ± AlF_3	0
Lewis acid–base pairs	
Fig. 1b	−7.36
Fig. 1c	−2.58
Transition structures	
Fig. 2a	99.23
Fig. 2b	50.22
Product formation	
$CF_3CFO + CF_3CF_3 \pm AlF_3$	2.53

All energies are relative to the reactant, and corrected for zero-point energies.

3.2. Skeletal degradation of PFDEE

Experimental data indicate that the formation of Lewis acid sites will catalyze the degradation of PPFE lubricants [2–7]. A commonly accepted decomposition mechanism centers around a reaction occurring at the $-OCF_2-$ linkage resulting in loss of small molecule products such as COF_2, and formation of –CFO at the ends of broken chains [2–4,15–17]. We examine several plausible degradation reaction paths leading to the formation of such products. First, the high shear rates produced by slider-disk contact could lead to radical formation in the polyperfluorinated ether lubricant by mechanically induced bond scissions [16]. Second, if the ether oxygen atoms in PPFE are interacting with Lewis acid sites, there is a weakening of the adjacent C–O bonds, as discussed above, possibly leading to a bond scission. Thus, we consider a simple C–O bond scission, as shown in Eq. (1). Finally, the interdigitation within PPFE structures allows relatively small non-bond interatomic distances, for example, 2.7 Å for C6–F5 (see Fig. 1a), setting up a possible transfer of a fluorine atom (such as F5 to C6), as shown in Fig. 2a, and summarized in Eq. (2).

$$CF_3CF_2OCF_2CF_3 \rightarrow CF_3CF_2O^{\cdot} + {}^{\cdot}CF_2CF_3 \quad (1)$$

$$CF_3CF_2OCF_2CF_3 \rightarrow \text{Fig. 2a} \rightarrow CF_3CFO + C_2F_6 \quad (2)$$

Formation of the –CFO end group at the ends of scissioned chains, as shown in Eq. (2), is among the major chemical changes that occur in the catalytically induced degradation of PPFE materials [2–6]. Therefore, we first consider the decomposition of PFDEE via a transition structure such as shown in Eq. (2).

3.2.1. The decomposition of PFDEE via a transition structure

The optimized structural parameters for the transition structure, Fig. 2a, are summarized in Table 2. The most significant change in the geometry of Fig. 2a, compared to PFDEE, arises from the interaction of the F5 fluorine atom with the electron deficient C6 atom in Fig. 2a. The formation

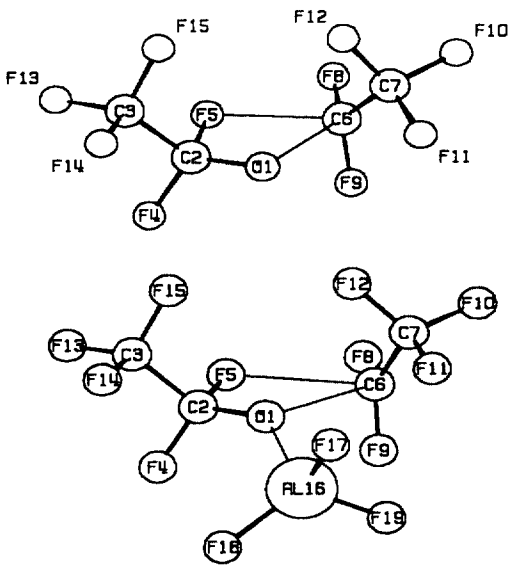

Fig. 2. HF/6-31G* optimized geometries.

of the local cyclization by the atoms C2, O1, C6, and F5, may be interpreted as a precursor to a decomposition reaction involving a fluorine atom transfer between F5 and C6, together with the scissioning of the C6–O1 and C2–F5 bonds, and the formation of a C2–O1 double bond. The new bond to be formed, F5–C6, computed to be 2.09 Å at the transition state, is considerably shorter than the non-bond distance of 2.96 Å computed for the initial PFDEE structure (Fig. 1a). The scissioning bond in the transition structure Fig. 2a, O1–C6, is computed to be 2.36 Å, considerably longer than the original 1.36 Å computed for PFDEE. The other scissioning bond, C2–F5, computed to be 1.49 Å at the transition structure, is appreciably longer than the 1.32 Å computed for PFDEE. The F5–C2–O1–C6 dihedral angle is near 9°, indicative of a non-planar geometry within the cyclic transition structure. At the transition geometry, the weakening of the C2–F5 and O1–C6 bonds, concomitant with the increased interaction between F5 and C6, causes a new bond to be formed between F5 and C6, and a scissioning of the O1–C6 and C2–F5 bonds, producing CF_3CF_3 and CF_3CFO.

The relevant bond orders computed at SCF/6-31G* are considered in Table 3. At the transition structure, the C2–O1 bond order of 1.40 is much larger than the corresponding ether, 0.86, indicative of a considerable structural shift towards a more double bond-like C=O as might be expected for a subsequent product like CF_3CFO. Both the O1–C6 and C2–F5 bond orders in the transition structure have decreased considerably compared to PFDEE, from 0.86 to 0.15 and 0.92 to 0.53, respectively, indicative of a considerable weakening of these bonds. Concomitantly, the bond order for the emerging F5–C6 bond has increased from the nearly zero 0.002 to the small but significant 0.20. All of these geometric changes at the transition state are indicative that the transition structure will produce CF_3CFO and CF_3CF_3.

The transition state structure was further characterized by computing the second derivatives at the optimized geometry,

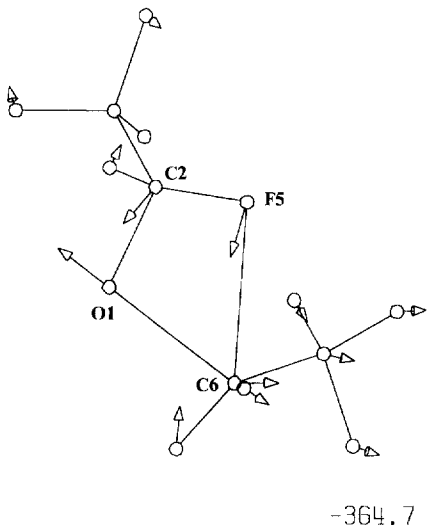

Fig. 3. HF/6-31G* normal mode displacement vectors for the imaginary frequency of the transition structure shown in Fig. 2a.

Fig. 3. One imaginary frequency was computed at 365i cm^{-1}, unscaled, at the SCF/6-31G* geometry. The normal mode displacement vectors correspond to C2–O1, C6–O1 and C6–F5 stretching vibrations, connecting reactant to the products CF_3CFO and C_2F_6.

The intramolecular interactions at the transition state are also summarized in Table 4 in terms of the computed partial atomic charges. Relative to PFDEE, F5 at the Fig. 2a transition state is significantly more basic and hence interacts more strongly with the electropositive C6 carbon atom. The oxygen atom O1 in Fig. 2a is significantly more negative than in PFDEE, indicative of an availability for bonding. As a result, the C2, F4, and O1 local structure begins to resemble the perfluoroacetaldehyde –CFO at the transition geometry.

Formation of the formal F5–C6 bond concomitant with the scissioning of the O1–C6 and C2–F5 bonds leads to the formation of the CF_3CFO and CF_3CF_3 products. As shown in Table 5, the decomposition of $CF_3CF_2OCF_2CF_3$ to CF_3CFO and CF_3CF_3 is computed to be slightly endothermic, 2.5 kcal/mol. The computed results also indicate that the SCF calculations using the 6-31G* basis set predict a larger activation energy for attaining the Fig. 2a transition structure, compared to either a C–C or C–O bond scission. These results mirror the SCF results obtained at the 6-31G* basis set for the decomposition of CF_3OCF_3 to COF_2 and CF_4. We alert the reader that in those studies, it was shown that the use of correlated wavefunctions placed the activation energy for the transition state approximately 20 kcal/mol lower in energy than for the corresponding C–O bond scission [9]. By analogy, we may have expected a similar finding here had correlated wavefunctions been employed. More importantly, the results in Table 5 indicate that, regardless of whether the reaction coordinate proceeds by a transition state or by free radicals initiated by a bond scission, a fairly large activation energy, $\simeq$73–99 kcal/mol, separates reactant and product. These results partially explain why polyperfluorinated ethers intrinsically enjoy thermal stability.

3.2.2. The effect of AlF_3 on the decomposition of PFDEE via a transition structure

The optimized geometry for the transition state structure connecting the reactant PFDEE to products CF_3CFO and CF_3CF_3, while interacting with an AlF_3 substrate, is presented in Fig. 2b. The optimized structural parameters are summarized in Table 2. As a result of the Lewis acid–base interaction, the O1–C6, C2–O1, and F5–C6 bonds in Fig. 2b are 0.36, 0.05, and 0.24 Å longer than the corresponding bonds in Fig. 2a. The C2–F5 bond is shorter in Fig. 2b, 1.402 Å compared to 1.486 in Fig. 2a. These results are indicative that the transition geometry Fig. 2b has retained a greater local ether structure about the C2, O1 atoms compared to a perfluoroacetaldehyde local geometry, Fig. 2a. In addition, we find that the O1–C6 bond in Fig. 2b is considerably longer than the corresponding bond in Fig. 2a, compensated for by the formation of a strong O1–Al16 bond. The oxygen–aluminum bond, 1.85 Å, is significantly shorter in the Fig. 2b transition structure compared to the sterically limited value of 2.54 Å computed for PFDEE–AlF_3 in Fig. 1c. In the transition structure shown in Fig. 2b, the terminal perfluoromethyl groups are rotated out of the local plane by approximately 50°, exposing the ether oxygen atom to the AlF_3 surface. The computed bond orders, Table 3, corroborate the increased strength of the oxygen–aluminum bond, and the severely weakened O1–C6 ether bond.

The computed F5–C6 interatomic distance is 2.33 Å, and has lengthened considerably in Fig. 2b, compared to the computed 2.09 Å in Fig. 2a. However, the F5–C6 bond order in Fig. 2b is 0.10, considerably larger than the non-bond 0.002 computed for PFDEE, indicative of interaction between these two atoms at the transition geometry despite the increased distance.

A summary of the activation energies is presented in Table 5. The activation energy for Fig. 2b, relative to the reactants, is 50 kcal/mol, approximately 50% less than for the corresponding transition structure in the absence of the Lewis acid–base interaction, 99 kcal/mol. Thus, the presence of Lewis acids such as AlF_3 is observed to significantly facilitate the decomposition of polyperfluorinated ethers via the cyclic transition state, by changing the reaction path along the decomposition reaction coordinate.

3.2.3. Decomposition of PFDEE via radical formation

We now consider the decomposition reactions of PFDEE initiated by radicals after an initial C–O bond scission, Eq. (1). An initial C–O bond scission of PFDEE produces the $CF_3CF_2^{\bullet}$ and $^{\bullet}OCF_2CF_3$ radicals which proceed with a bond scission energy of 72 kcal/mol. Fluorine abstraction by $CF_3CF_2^{\bullet}$ from $^{\bullet}OCF_2CF_3$ produces C_2F_6 and CF_3CFO. The ΔH at 298 K for the reaction $CF_3CF_2OCF_2CF_3$ to produce the products C_2F_6 and CF_3CFO is 3 kcal/mol, Table 6. Alternatively, after the formation of the $CF_3CF_2^{\bullet}$ and $^{\bullet}OCF_2CF_3$ radicals, the $^{\bullet}OCF_2CF_3$ radical itself may undergo scissioning to produce other possible products. For example, $CF_3CF_2O^{\bullet}$ may decompose by either a C–C or a C–F bond scission. The

Table 6
The ΔH and ΔG values at 298 K computed at SCF/6-31G*

Reaction	$\Delta H_{298\ K}$ kcal/mol	$\Delta G_{298\ K}$ kcal/mol
Overall product formation reactions		
$CF_3CF_2OCF_2CF_3 \rightarrow C_2F_6 + CF_3CFO$	+3.0	−10.6
$CF_3CF_2OCF_2CF_3 \rightarrow C_3F_8 + COF_2$	+3.6	−9.0
Radical reactions from initial C–O cleavage		
$CF_3CF_2OCF_2CF_3 \rightarrow CF_3CF_2^{\bullet} + {}^{\bullet}OCF_2CF_3$	+72.7	
$CF_3CF_2O^{\bullet} \rightarrow COF_2 + CF_3^{\bullet}$	2.9	
$CF_3CF_2O^{\bullet} \rightarrow CF_3CFO + F^{\bullet}$	18.3	

All energies are in kcal/mol and corrected for zero-point contributions.

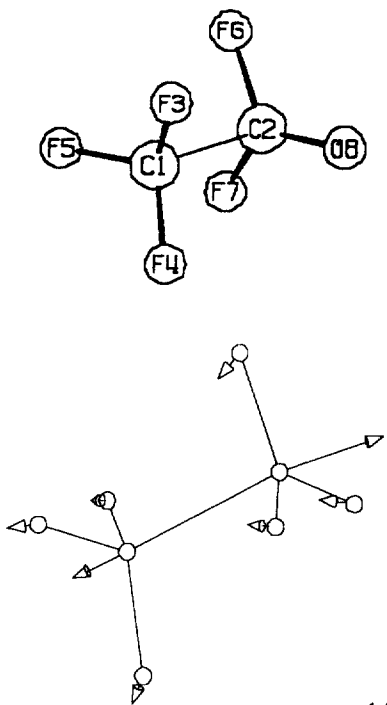

Fig. 4. HF/6-31G* optimized geometry for the $CF_3\cdots CF_2O^{\bullet}$ transition structure. The corresponding normal mode displacement vectors for the imaginary frequency of the transition structure is shown below.

Table 7
The relative total energies (6-31G*) for the various structures in kcal/mol

Structure	ΔE (kcal/mol)
Reactant	
$CF_3CF_2O^{\bullet}$	0
Transition structure	
$CF_3\cdots CF_2O$ (Fig. 4)	24.35
Product formation	
$CF_3^{\bullet} + COF_2$	2.36

All energies are relative to the reactant, and corrected for zero-point energies.

results of the ab initio calculations clearly show that the C–C scission is energetically favored, $\Delta H_{298\ K} = 2.9$ kcal/mol to form COF_2 and $CF_3^{\bullet}$ compared to 18.3 kcal/mol to produce CF_3CFO and $F^{\bullet}$. We have computed the transition structure, and hence the activation energy, for the decomposition of $CF_3CF_2O^{\bullet}$ to $CF_3^{\bullet} + COF_2$. The optimized geometry is shown in Fig. 4 along with the normal mode vectors associated with the imaginary frequency. The C1–C2 bond length is 1.975 Å, indicative of a scissioning bond. The C2–O8 bond length is 1.209 Å, intermediate between the 1.16 Å computed for carbonyl fluoride [17], and the 1.35 Å computed for the $CF_3CF_2O^{\bullet}$ radical. Hence, the C2, F6, F7, and O8 atoms have already began to locally form COF_2. The activation energy to form the transition structure, Fig. 4, is 24.4 kcal/mol, Table 7. Such a comparatively low activation energy would allow the facile decomposition of polyperfluorinated ethers that have the $-CF_2O-$ monomer units at the radical sites.

4. Concluding remarks

Lewis acid catalysis significantly enhances the thermally induced degradation of polyperfluorinated ether lubricants. Using $CF_3CF_2OCF_2CF_3$ and AlF_3, we have characterized several model Lewis acid–base interactions between PFDEE and AlF_3. The results of these studies indicate that perfluorodiethyl ether, or PFDEE, may form a Lewis acid–base pair between the ether oxygen atom in PFDEE and the aluminum atom in AlF_3 provided that there is no steric hindrance limiting access to the ether oxygen atom. This may be achieved, for example, by PFDEE adopting a trans–gauche instead of a trans–trans conformation. In the trans–trans conformation, a terminal perfluoromethyl group sterically interferes with the accessibility of the ether oxygen atom to the AlF_3 surface. These results indicate that in lubricant molecules such as the 'Z' family of Fomblin fluids, composed of a copolymer of perfluoromethylene and perfluoroethylene oxide units, steric hindrance will limit AlF_3 access to the ether oxygen atom when $-CF_2CF_2OCF_2CF_2-$ structural units prevail in a trans–trans configuration. For the $-CF_2CF_2OCF_2CF_2-$ structural unit to interact effectively with the AlF_3 surface, an internal rotation about the C–C–O–C would be required. On the other hand, the interaction between the ether oxygen and aluminum atoms in the $-CF_2-O-CF_2-$ local structure is expected to proceed with little or no steric hindrance and hence, will represent the weakest link, with respect to catalytic degradation, in the Z family of polyperfluorinated ethers. These results therefore explain at the molecular level why polyperfluorinated ether lubricants exhibit increased stability to Lewis acid-induced degradation as the number of carbon atoms between the ether oxygen atoms increase. Even when the PFDEE backbone adopts a local trans–gauche conformation such as to allow a Lewis acid–base interaction between the ether oxygen atom and aluminum, the interatomic distance is much greater, 2.5 Å compared to 1.8 Å for

perfluoromethylene oxide. The binding energy is correspondingly smaller, −3 compared to −9 kcal/mol, respectively.

Several degradation paths for the decomposition of PFDEE, originating within the $-CF_2OCF_2-$ structural group, were computed. Thus, the decomposition of PFDEE to CF_3CF_3 and CF_3CFO via an initial cleavage of a C–O bond, and, alternatively, via a concerted reaction through the formation of a cyclic transition state, were investigated. In both cases, the activation energy to initiate the decomposition is rather high, near 80–100 kcal/mol. However, in the presence of an AlF_3 catalyst, the activation energy for the concerted reaction is significantly reduced, by approximately 50% to 50 kcal/mol. Thus, exposure of the $-CF_2OCF_2-$ structural units to Lewis acids is undoubtedly the weak link in the Z family of polyperfluorinated ether lubricants.

References

[1] R.J. Waltman, D. Pocker, G. Tyndall, Tribol. Lett., in press (1998).
[2] P.H. Kasai, P. Wheeler, Appl. Surf. Sci. 52 (1991) 91.
[3] P. Kasai, Macromolecules 25 (1992) 6791.
[4] P. Kasai, W.T. Tang, P. Wheeler, Appl. Surf. Sci. 51 (1991) 201.
[5] S. Mori, N. Onodera, Wear 168 (1993) 85.
[6] S. Mori, W. Morales, Wear 132 (1989) 111.
[7] A. Hess, E. Kemnitz, J. Catal. 149 (1994) 449.
[8] J. Pacansky, R.J. Waltman, J. Fluorine Chem. 82 (1997) 79.
[9] J. Pacansky, R.J. Waltman, J. Fluorine Chem. 83 (1997) 41.
[10] B.H. Lengsfield, H. Horn, A.D. McLean, J.T. Carter, E.S. Replogle, L.A. Barnes, S.A. Maluendes, G.C. Lie, J.E. Rice, M. Gutowski, W.E. Rudge, S.P.A. Sauer, R. Lindh, K. Andersson, T.S. Chevalier, P.-O. Widmark, D. Bouzida, G. Pacansky, K. Singh, C.J. Gillan, P. Carnevali, W.C. Swope, B. Liu, Mulliken 2.0, Almaden Research Center, IBM Research Division, 6500 Harry Road, San Jose, CA 95120-6099.
[11] K. Raghavachari, J.A. Pople, Int. J. Quant. Chem. 20 (1981) 1067.
[12] S.D. Williams, W. Harper, G. Mamantov, L.J. Tortorelli, G. Shankle, J. Comput. Chem. 17 (1996) 1696.
[13] J. Pacansky, M. Miller, W. Hatton, B. Liu, A. Scheiner, J. Am. Chem. Soc. 113 (1991) 329.
[14] G.D. Smith, R.L. Jaffee, D.Y. Yoon, Macromolecules 28 (1995) 5804.
[15] J. Pacansky, R.J. Waltman, Chem. Mater. 5 (1993) 1526.
[16] B.D. Strom, D.B. Bogy, R.G. Walmsley, J. Brandt, C.S. Bhatia, Wear 168 (1993) 31.
[17] J. Pacansky, R.J. Waltman, Y. Ellinger, J. Phys. Chem. 98 (1994) 4787.